nature climate change

LETTERS

PUBLISHED ONLINE: 21 DECEMBER 2015 | DOI: 10.1038/NCLIMATE2873

Multi-scale predictions of massive conifer mortality due to chronic temperature rise

N. G. McDowell[1]*, A. P. Williams[1,2], C. Xu[1], W. T. Pockman[3], L. T. Dickman[1], S. Sevanto[1], R. Pangle[3], J. Limousin[3], J. Plaut[3], D. S. Mackay[4], J. Ogee[5], J. C. Domec[5,6], C. D. Allen[7], R. A. Fisher[8], X. Jiang[8†], J. D. Muss[1], D. D. Breshears[9], S. A. Rauscher[10] and C. Koven[11]

Global temperature rise and extremes accompanying drought threaten forests[1,2] and their associated climatic feedbacks[3,4]. Our ability to accurately simulate drought-induced forest impacts remains highly uncertain[5,6] in part owing to our failure to integrate physiological measurements, regional-scale models, and dynamic global vegetation models (DGVMs). Here we show consistent predictions of widespread mortality of needleleaf evergreen trees (NET) within Southwest USA by 2100 using state-of-the-art models evaluated against empirical data sets. Experimentally, dominant Southwest USA NET species died when they fell below predawn water potential (Ψ_{pd}) thresholds (April–August mean) beyond which photosynthesis, hydraulic and stomatal conductance, and carbohydrate availability approached zero. The evaluated regional models accurately predicted NET Ψ_{pd}, and 91% of predictions (10 out of 11) exceeded mortality thresholds within the twenty-first century due to temperature rise. The independent DGVMs predicted ≥50% loss of Northern Hemisphere NET by 2100, consistent with the NET findings for Southwest USA. Notably, the global models underestimated future mortality within Southwest USA, highlighting that predictions of future mortality within global models may be underestimates. Taken together, the validated regional predictions and the global simulations predict widespread conifer loss in coming decades under projected global warming.

Forest mortality has been widely documented in recent years[1,2,7,8] and has accelerated in concert with rising CO_2 and temperature[2,7] (Fig. 1a and Supplementary Information 1). The terrestrial carbon sink could be severely diminished over the next century if this acceleration of tree mortality continues with warming and increased extreme drought events[5,9], causing a positive feedback on global warming[3,10]. Predictions of the terrestrial carbon sink vary markedly across models (for example, ref. 5) in part because the mechanisms of tree death are still poorly understood[6] and thus forecasts remain largely speculative.

Here we demonstrate that predawn plant water potential (Ψ_{pd}), through its impact on canopy-scale stomatal conductance (G_s) and regulation of carbon and water balance, is a key predictive element to mechanistically represent vegetation mortality. We extend this analysis to include multiple process-based and empirical models to investigate the likelihood of future mortality of needleleaf evergreen trees (NET) in Southwest USA. We then compare these results with those from the dynamic global vegetation models (DGVMs) from the CMIP5 (Coupled Model Intercomparison Project, Phase 5) to examine whether completely independent simulations provide similar predictions for the NET biome as predicted for Southwest USA. This last step further allows comparison within the Southwest USA of the un-evaluated and less mechanistic DGVM predictions against the evaluated simulations of the regional models.

Plants must balance multiple demands on stomatal control during drought: severe water potential declines promote hydraulic failure[11], while G_s reductions limit this decline and minimize the risk of hydraulic failure but thus inhibit CO_2 diffusion into leaves[12]. G_s decline *per se* does not induce mortality, but theory and evidence point to drought-induced declines in hydraulic function and photosynthesis (through G_s decline) as the primary drivers of death because of their downstream impacts leading to carbon starvation, hydraulic failure, and biotic attack, particularly if G_s is low for long durations[6,13–17]. The G_s response to drought varies across the isohydry–anisohydry continuum of hydraulic strategies[18] (Fig. 1b and Supplementary Information 2). Across this continuum of hydraulic strategies, G_s declines with decreasing soil water potential (Ψ_s) or leaf water potential (Ψ_l), decreasing hydraulic conductance (k), and increasing vapour pressure deficit (D) (ref. 19, Fig. 1b):

$$G_s = \frac{k(\Psi_s - \Psi_l)c}{D} \quad (1)$$

Equation (1), where c is a coefficient representing air and water thermodynamic properties, is a simplified model (Supplementary Information 3) that illustrates the dependence of G_s, and therefore photosynthesis, on drought-induced declines in k (which declines along the continuum of hydraulic failure during drought), Ψ_s, and increasing D (the atmospheric driving force for transpiration). Equation (1) has been validated in numerous studies (Supplementary Information 3), and assumes steady-state conditions and adequate coupling between the canopy and the atmosphere (reviewed in Supplementary Information 3 and in

[1]Earth and Environmental Sciences Division, MS-J495, Los Alamos National Lab, Los Alamos, New Mexico 87545, USA. [2]Lamont-Doherty Earth Observatory, Columbia University, Palisades, New York 10964, USA. [3]Biology Department, University of New Mexico, Albuquerque, New Mexico 87131, USA. [4]Department of Geography, University at Buffalo, Buffalo, New York 14260, USA. [5]UMR 1391 ISPA, INRA-Bordeaux Sciences Agro, Villenave d'Ornon 33140, France. [6]Nicholas School of the Environment, Duke University, Durham, North Carolina 27708, USA. [7]US Geological Survey, Fort Collins Science Center, Jemez Mountains Field Station, Los Alamos, New Mexico 87544, USA. [8]National Center for Atmospheric Research, Boulder, Colorado 80305, USA. [9]School of Natural Resources and the Environment, and Department of Ecology and Evolutionary Biology, University of Arizona, Tucson, Arizona 85721, USA. [10]Department of Geography, University of Delaware, Newark, Delaware 19716, USA. [11]Earth Sciences Division, Lawrence Berkeley National Lab, 1 Cyclotron Road, Berkeley, California 94720, USA. †Present address: Department of Earth System Science, University of California, Irvine 92697, USA. *e-mail: mcdowell@lanl.gov

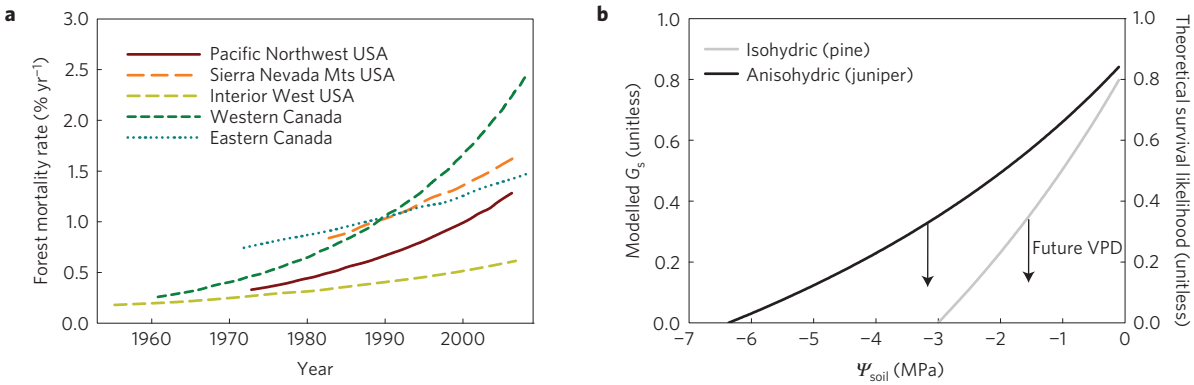

Figure 1 | Observations and theoretical drivers of increasing conifer mortality. a, Reported mortality observations are increasing throughout North America, across a mean annual precipitation range of 202–3,928 mm yr^{-1} and a mean annual temperature range of −5.7–12.0 °C (refs 2,7). **b**, Predictions of stomatal conductance and by inference, survival of relatively isohydric and anisohydric species, in response to decreasing soil water potential. Rising future D forces a shift downward in the curves, thereby reducing G_s and survival likelihood.

ref. 17). As survival depends on sustained maintenance of a net positive G_s (refs 6,12–17), equation (1) also suggests that mortality may increase when drought causes a sustained decrease in Ψ_s or k, and an increase in D (Fig. 1b). Rising D is potentially the largest threat to survival associated with climate change because global temperature rise is driving a chronic rise in D despite concurrent increases in specific humidity[20] (Supplementary Information 4).

We first combined observational and experimental data sets with models (using both published and unpublished data and simulations[13]) to examine the likelihood of future mortality and survival for piñon pine and juniper trees (*Pinus edulis* and *Juniperus monosperma*) in Southwest USA. In a field experiment, we removed ~48% of ambient rainfall from three 1,600 m^2 plots for five years in a piñon–juniper woodland in central New Mexico, USA (Supplementary Information 5). We made measurements of Ψ_{pd}, G_s and other variables critical to plant survival during drought[6]. Across the three drought plots, the mature (>100 years old) piñon pine experienced ~80% whole-tree mortality; trees with April–August mean (growing season[20]) Ψ_{pd} averaging −2.4 MPa or lower all died (Fig. 2a and Supplementary Information 5). Crown dieback of juniper started after a continuous April–August period with Ψ_{pd} below −5.3 MPa, resulting in ~50% canopy loss and approximately 25% whole-tree mortality. The Ψ_{pd} value associated with mortality was consistent with the Ψ value associated with zero G_s and zero photosynthesis (Ψ_{A0}) for each species (Fig. 2b,c, see Supplementary Information 6 for all regression statistics from Fig. 2). Consistent exceedance of Ψ_{pd} below Ψ_{A0} during April–August (that is, maintaining negative Ψ_{A0} values) resulted in downstream consequences on the physiology of both species, including severe levels of hydraulic failure (percentage loss of whole-tree conductance; Fig. 2d), near-zero whole-tree k (Fig. 2e), and reductions in foliar starch (Fig. 2f). Extreme values in Fig. 2b–f were consistent with the Ψ_{pd} mortality thresholds for each species (Fig. 2a). Additionally, formation of resin ducts for defence against biotic attack declined to nearly zero in the pine trees that died but remained high for those that survived[21]. Therefore, all potential mechanisms of mortality reached similarly critical values at or before species-specific Ψ_{A0} values (Fig. 2 and Supplementary Information 7).

The Ψ_{pd} mortality thresholds identified from the drought experiment (Fig. 2) validated well against the world's longest continuous Ψ_{pd} record, also for piñon pine and juniper trees in New Mexico (an extension of refs 22,23; Supplementary Fig. 1A). Using this long-term data set, we assessed whether precipitation and D predicted by the CMIP5 multi-model ensembles could be used to infer our long-term Ψ_{pd} observations (1992–2013). Observed annual precipitation and D together explain 70 and 80% of the annual variation in growing-season mean Ψ_{pd} for pine and juniper, respectively, at the long-term observational site (Supplementary Fig. 1). An independent test against the drought manipulation site (Fig. 2) also produced a strong predictive relationship for both species (Supplementary Figs 1 and 2).

The strength of empirical models (for example, equations Supplementary Information 2 and 3) is that they reflect the observations without need to simulate processes; however, they may not capture future nonlinearity—in this case, responses to a future world with higher temperature, D and CO_2. We investigated simulations by the process-based models TREES, MuSICA and ED(X) that account for nonlinear effects of changes in these variables (see Supplementary Information 8 and Supplementary Fig. 3). After model tuning (Supplementary Information 7) each model simulated each species Ψ_{pd} as accurately as the empirical model (Supplementary Fig. 2).

The 'business-as-usual' greenhouse gas emissions scenario (RCP 8.5) from CMIP5 suggests that by AD 2100, precipitation will decrease by 10% and D will increase by 33% in Southwest USA (compared with year 2000; Fig. 3a,b). Using these climate projections to drive the empirical and process-based models resulted in relatively consistent predictions of declining Ψ_{pd} over time for both piñon and juniper (Supplementary Figs 4 and 5), falling below the Ψ_{A0} threshold for both species by 2020–2060 (Fig. 3c and Supplementary Fig. 4). This outcome is delayed by approximately one decade when RCP 4.5, a more optimistic greenhouse gas reductions scenario, is used (Supplementary Fig. 6). These predictions are consistent with NET losses for a tree-ring-based forest drought stress model[20] and for both Southwest and northwest USA from the Community Earth System Model[24] (CESM; Fig. 3c). Averaging all models shown in Fig. 3c suggests that 72% of the regions NET forests will experience mortality by 2050, with nearly 100% mortality of Southwest USA forests by 2100.

The simulations shown in Fig. 3c suggest that Southwest NET species, even the particularly drought-tolerant piñon pine and juniper trees, are likely to experience widespread mortality before 2100. Substantial documented piñon mortality in the early 2000s (refs 1,20,22,23) and widespread observations of recent juniper mortality (Supplementary Fig. 1B) in Southwest USA are consistent with this result, despite juniper's reputation as being this region's most drought-tolerant conifer[23]. We note that all predictions shown in Fig. 3c are independent except for their use of CMIP5 ensemble climate forecasts. ED(X), the most conservative model, predicted two less severe trends (Fig. 3c). First, ED(X) indicated that juniper could survive well into the twenty-second century (Fig. 3c) owing in part to juniper's particularly low vulnerability to cavitation, which is rare amongst the NET plant functional type[25]. Second, ED(X)

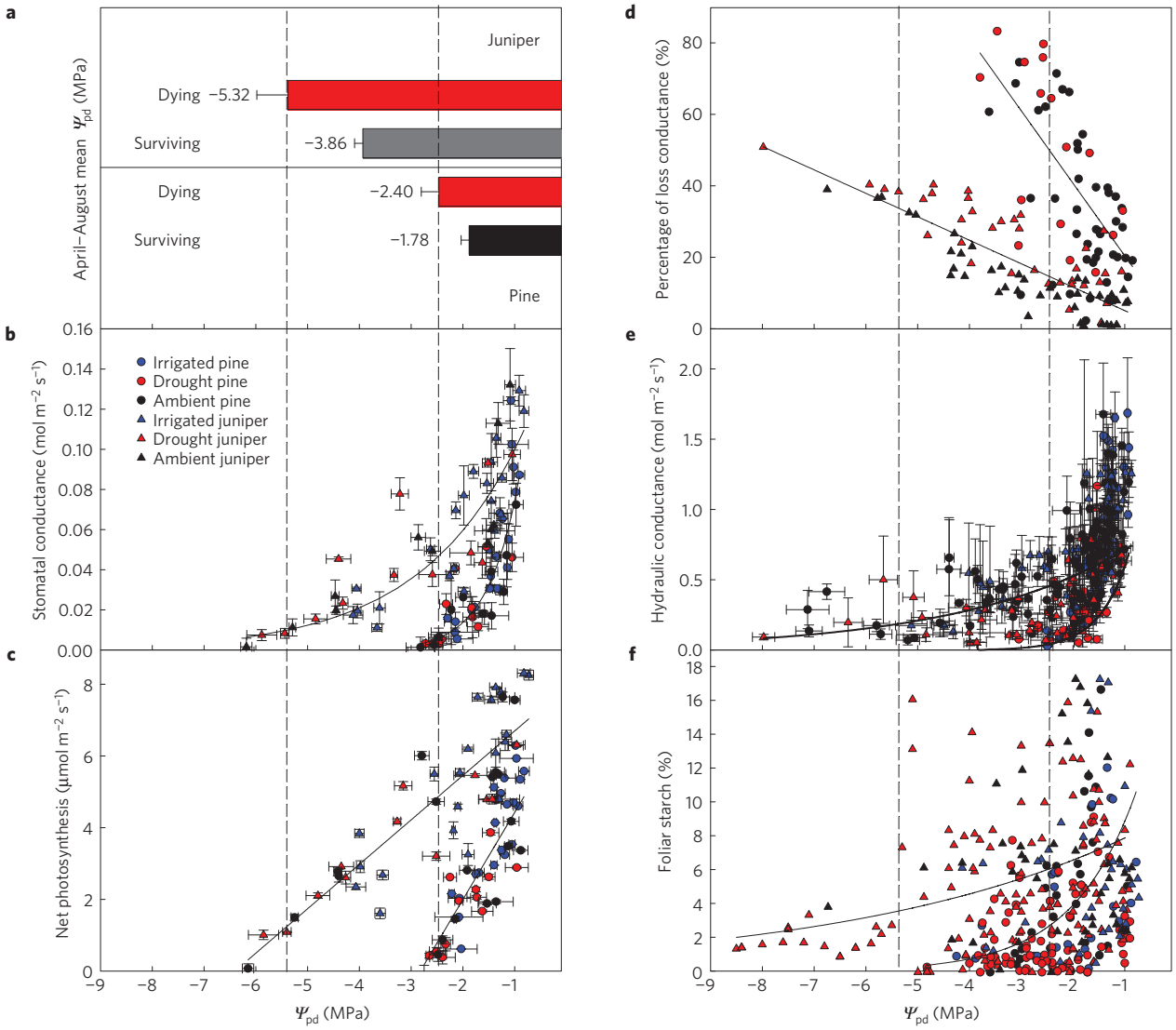

Figure 2 | Predawn Ψ measurements are strongly correlated with the mechanisms of mortality[6]. a, Trees that die of each species averaged more negative Ψ from April to August than trees that survived ($p < 0.01$ for both species). Vertical lines demark thresholds for pine and juniper. **b**–**f**, Stomatal conductance (**b**), net photosynthesis (**c**), modelled whole-tree percentage loss of conductance (hydraulic failure) (**d**), measured whole-tree hydraulic conductance (**e**), and foliar starch (**f**) all declined with Ψ_{pd} for both species. Error bars are standard errors.

was run for 72 one-degree grid cells over Southwest USA (Fig. 3d), predicting that mortality will occur primarily in warmer southern locations. ED(X) results suggest that temperature is the primary driver of mortality through increasing D (Supplementary Fig. 7). Given the importance of temperature to tree survival, future forest management may take advantage of potential refugia in cooler landscape locations and planting of warm-adapted genotypes.

We placed our results for the Southwest USA into a global context through comparison to independent NET simulations for the Northern Hemisphere from four DGVMs that were run with dynamic vegetation enabled (Supplementary Information 9). This comparison allowed building of confidence in our predictions if the independent, non-evaluated DGVMs provided similar results for the NET biome at the global scale as those from the evaluated regional process models, and this further allowed direct regional comparison of the DGVMs to the evaluated and more detailed process model predictions for Southwest USA. The first three DGVM simulations are Earth system models (ESMs) from the CMIP5 archive that have interacting land–atmosphere–ocean dynamics, and are entirely independent of those shown in Fig. 3c, thus allowing us to examine the robustness of our predictions of NET loss under alternative modelled drivers and assumptions for climates outside the Southwest USA. These ESMs do not utilize the Ψ_{pd} thresholds identified in this analysis because such extrapolation of a model developed in Southwest USA to wetter, cooler regions of the NET biome, with other species and climate, may be inaccurate. These ESMs instead rely on the climate envelope and low-growth thresholds typical of DGVMs (ref. 6) making them largely independent of the Southwest USA simulations shown in Fig. 3c. All three ESMs simulated large NET losses throughout the temperate and southern boreal regions (−14.5 million km^2 on average; Fig. 4a–c; see Supplementary Information 10 for calculation explanation), although these are accompanied by NET gains in the northern boreal zones. Our fourth DGVM (CESM) simulated NET distributions to 2100 using coupled land–atmosphere dynamics forced by eight different sea surface temperature (SST) scenarios from fully coupled GCMs provided by CMIP3 (ref. 26). SST patterns play an important role in shaping how precipitation may change in a warmer world (for example, ref. 27); therefore, the use of different SSTs generates a range of potential future climate scenarios within the same model framework. The eight

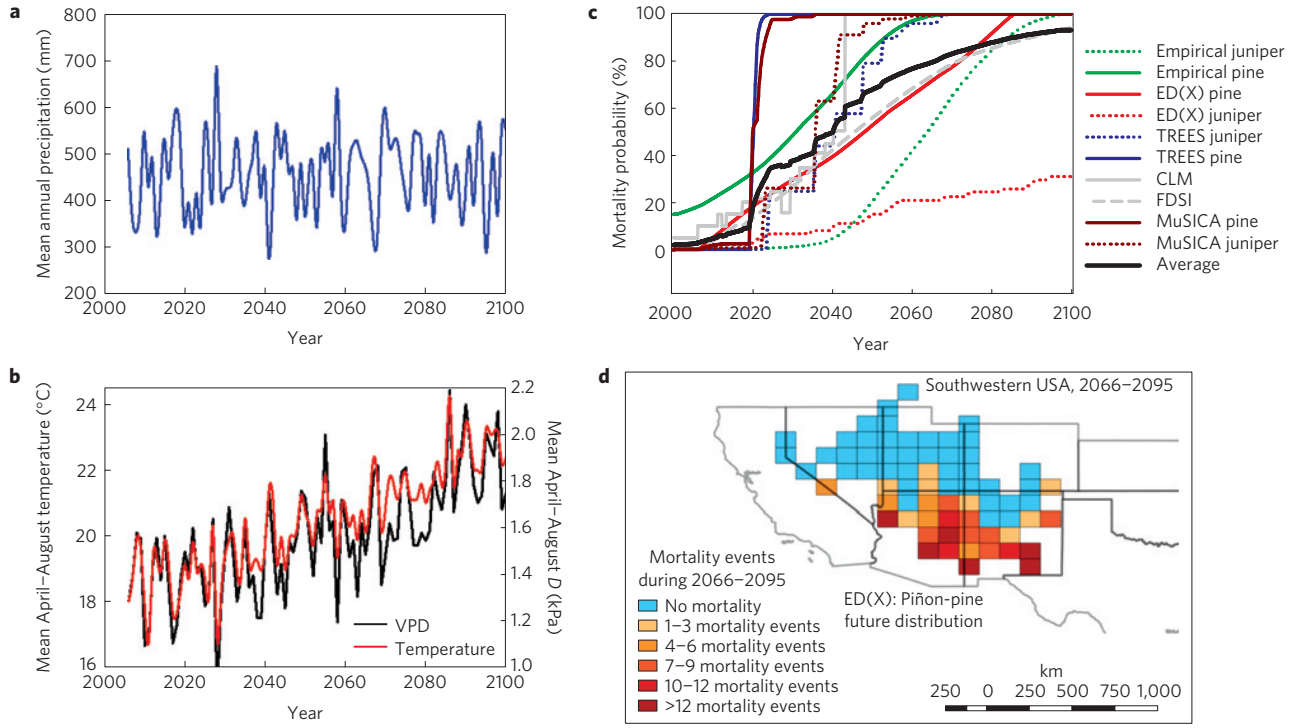

Figure 3 | Predictions of climate and forest mortality for Southwestern USA to AD 2100. a,**b**, Ensemble forecasts from CMIP5, RCP 8.5, of mean annual precipitation (**a**) and mean April–August vapour pressure deficit and temperature (**b**) for the distribution of pine–juniper woodlands in the Southwest USA. **c**, Predictions of the probability of future NET mortality events in the Southwest USA based on CMIP5 climate predictions and a variety of modelling approaches. Mortality was a function of simulated Ψ_{pd} exceeding Ψ_{A0} throughout April–August in the empirical model and ED(X), TREES, and MuSICA. CLM (ref. 24) used its own mortality algorithms and the Forest Drought Stress Index[20] used a threshold index based on historical observations. **d**, ED(X) simulations of the geographic pattern of pine–juniper mortality in the Southwest USA for RCP8.5 for the period 2066–2095. ED(X) simulations suggest that the southern half of the range is more likely to experience mortality than the northern half. This is particularly due to warming, with an apparent threshold warming of 1.95 °C (Supplementary Fig. 7). This regional heterogeneity may partially explain ED(X)'s relatively conservative mortality predictions (Fig. 3c).

simulations agreed that at least 50% of the NET plant functional type could be lost within the Northern Hemisphere by 2100, as indicated by the red swath across the temperate zone (Fig. 4d). Therefore, all four DGVMs and the more rigorous analysis for Southwest USA predict potential widespread NET mortality despite covering different regions and utilizing different mortality algorithms.

Despite the consistent predictions of widespread NET mortality highlighted in both Fig. 3c and Fig. 4a–d, a notable discrepancy emerges through comparison of the DGVM predictions of mortality in Southwest USA (Fig. 4e–h) with those of the validated ED(X) model (Fig. 3d). This may be caused by the lack of NET coverage in Southwest USA as prescribed by the DGVMs, by the DGVMs lumping of NET species into one plant functional type, and by their simplistic climate envelope and low-growth mortality thresholds. Assuming that the accuracy of the predictions in Fig. 3c is better than that of the DGVMs (because the models in Fig. 3c were developed and validated for this region), the discrepancy thus suggests that the DGVMs may be too conservative in their predictions of NET mortality, at least for Southwest USA, and provides motivation to improve the realism and evaluate the performance of future DGVM simulations. We note two additional caveats to the results shown in Fig. 4. First, global DGVM predictions have never been validated, so although their predictions represent the state of the art in global simulations, we cannot absolutely trust their outcomes to be realistic. Second, there are multiple processes not included in the models that could cause overestimates of future mortality, for example, by not accounting for acclimation, adaptation, and islands of refugia (such as those associated with beneficial topographic settings)[28]; or conversely underestimate future mortality by not including processes such as acceleration of insect population dynamics, increases in frequency and severity of wildfires, or failure of seedling recruitment[6,20,28].

The general agreement of rising mortality rates of the NET biome located within Southwest USA (Fig. 3), western and boreal North America[2,7] (Fig. 1a), and the Northern Hemisphere (Fig. 4), based on models and data sets with very different sets of assumptions and mechanisms, suggests a high likelihood that widespread mortality of NET forests will occur by 2100. The recently accelerating NET mortality rates are associated with warming[2,7,29] (for example, Supplementary Fig. 7). The rise in juniper mortality likelihood has alarming implications for conifers in general because juniper historically experienced far less mortality than other conifers during droughts[1,13,22,23]. The consequences of such broad-scale change in forest cover are substantial, including massive transfer of carbon to a decomposable pool[10] and changes in the surface energy budget[3,4]. The carbon consequences of tree mortality across the NET biome averaged 10 Pg C for the models shown in Fig. 4a–c, which is equivalent to predicted boreal carbon loss over the next century[30]. The projections are more optimistic for the far northern latitudes (Fig. 4); however, these boreal systems have lower carbon fluxes than most temperate zone forests.

These simulations of climate-induced vegetation change (Fig. 3c) are among the most rigorously tested by both experimental and observational data sets of physiological conditions associated with tree mortality. The ensemble analyses in this study consistently highlight vulnerability to collapse of the NET biome across many parts of the globe in coming decades, driven by warming temperatures and associated drought stress. Such rapid and extensive forest losses are likely to have profound impacts on carbon storage, climate forcing, and ecosystem services[31].

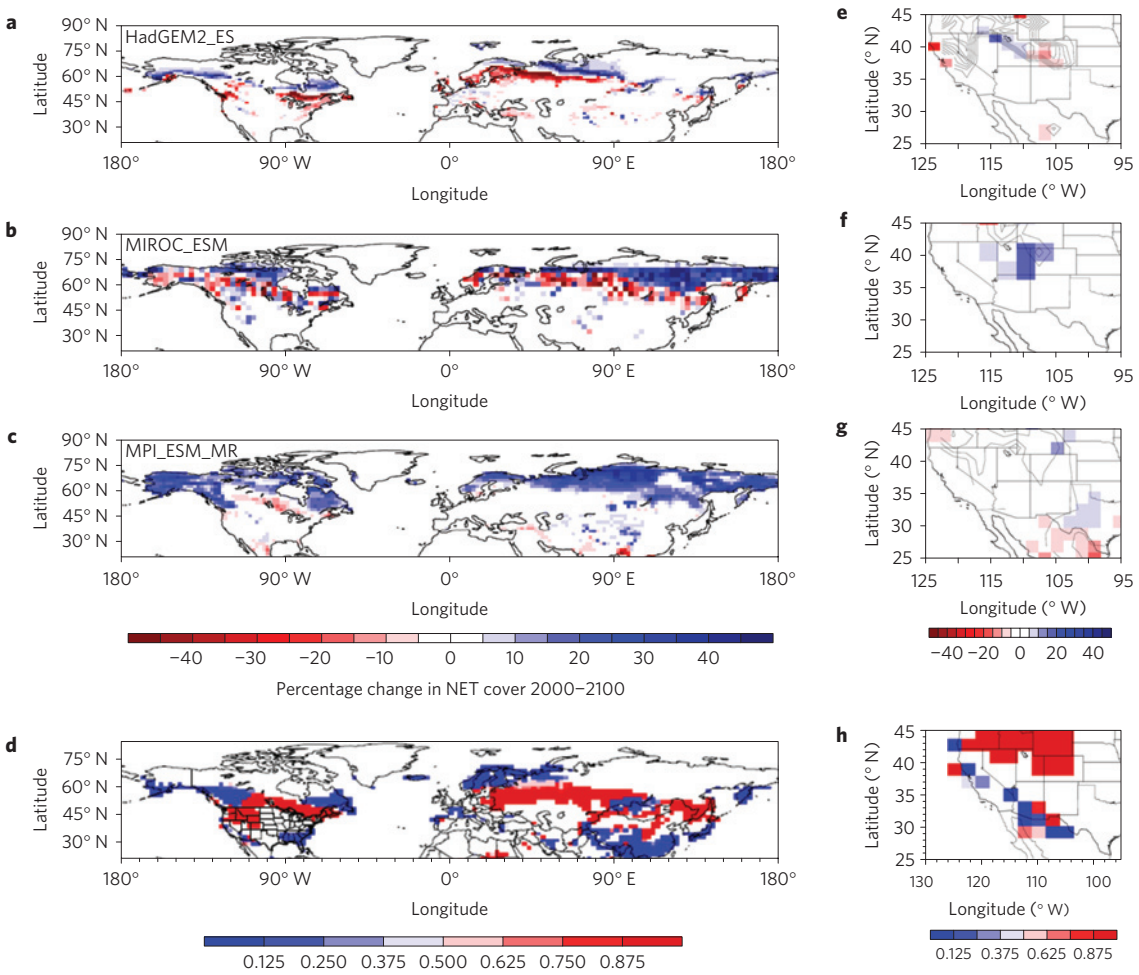

Figure 4 | Dynamic global vegetation models predictions of NET percentage losses between 2000 and 2100. a, HadGem2. **b**, MIROC_ESM. **c**, MIP_ESMLR. **d**, CESM. **a**–**c** show the percentage change in NET cover between 2000 and 2100. **d**, The fraction of eight CESM runs with different SST warming patterns, showing the model agreements that at least 50% of NET cover will be lost by 2100. **e**–**h**, Blow-ups of **a**–**d** for Southwestern USA, intended for comparison to Fig. 3d. **e**–**g** are HadGem2, MIROC_ESM, MPI_ESMLR with no change in representation of the results. Isolines in **e**–**g** show current NET distributions (in 10% coverage increments). **d** and **h** are presented as the fraction of models that simulate a 50% decrease in NET coverage, to allow more direct comparison to Fig. 3d. All simulations are independent of those done for Southwest USA.

Received 15 September 2014; accepted 25 September 2015; published online 21 December 2015; corrected after print 7 October 2016

References

1. Allen, C. D. *et al.* A global overview of drought and heat-induced tree mortality reveals emerging climate change risks for forests. *For. Ecol. Manage.* **259,** 660–684 (2010).
2. Peng, S. *et al.* A drought-induced pervasive increase in tree mortality across Canada's boreal forest. *Nature Clim. Change* **1,** 467–471 (2011).
3. Bonan, G. B. Forests and climate change: Forcings, feedbacks, and the climate benefits of forests. *Science* **320,** 1444–1449 (2008).
4. Maness, H., Kushner, P. J. & Fung, I. Summertime climate response to mountain pine beetle disturbance in British Columbia. *Nature Geosci.* **6,** 65–70 (2012).
5. Friedlingstein, P. *et al.* Uncertainties in CMIP5 climate projections due to carbon cycle feedbacks. *J. Clim.* **27,** 511–526 (2014).
6. McDowell, N. G. *et al.* Interdependence of mechanisms underlying climate-driven vegetation mortality. *Trends Ecol. Evol.* **26,** 523–532 (2011).
7. Van Mantgem, P. J. *et al.* Widespread increase of tree mortality rates in the western United States. *Science* **323,** 521–524 (2009).
8. Phillips, O. L. *et al.* Drought sensitivity of the Amazon rainforest. *Science* **323,** 1344–1347 (2009).
9. Reichstein, M. *et al.* Climate extremes and the carbon cycle. *Nature* **500,** 287–295 (2013).
10. Kurz, W. A. *et al.* Mountain pine beetle and forest carbon feedback to climate change. *Nature* **452,** 987–990 (2008).
11. Plaut, J. *et al.* Hydraulic limits preceding mortality in a piñon-juniper woodland under experimental drought. *Plant Cell Environ.* **35,** 1601–1617 (2012).
12. Cowan, I. R. & Givnish, T. J. *On the Economy of Plant Form and Function* 133–170 (Cambridge Univ. Press, 1986).
13. McDowell, N. G. *et al.* Evaluating theories of drought-induced vegetation mortality using a multi-model-experiment framework. *New Phytol.* **200,** 304–321 (2013).
14. Mitchell, P. J. *et al.* Drought response strategies define the relative contributions of hydraulic dysfunction and carbohydrate depletion during tree mortality. *New Phytol.* **197,** 862–872 (2013).
15. Poyatos, R. *et al.* Drought induced defoliation and long periods of near zero gas exchange play a key role in accentuating metabolic decline of Scots pine. *New Phytol.* **200,** 388–401 (2013).
16. Sevanto, S. *et al.* How do trees die? A test of the hydraulic failure and carbon starvation hypotheses. *Plant Cell Environ.* **37,** 153–161 (2013).
17. McDowell, N. & Allen, C. Darcy's law predicts widespread forest loss due to climate warming. *Nature Clim. Change* **5,** 669–672 (2015).
18. Martínez-Vilalta, J. *et al.* A new look at water transport regulation in plants. *New Phytol.* **204,** 105–115 (2014).
19. Whitehead, D. & Jarvis, P. G. in *Water Deficits and Growth* Vol. 6 (ed. Kozlowski, T. T.) 49–152 (Academic, 1981).
20. Williams, A. P. *et al.* Temperature as a potent driver of regional forest drought stress and tree mortality. *Nature Clim. Change* **3,** 292–297 (2013).

21. Gaylord, M. L. *et al.* Drought predisposes piñon-juniper woodlands. *New Phytol.* **198,** 567–568 (2012).
22. McDowell, N. G. *et al.* Mechanisms of plant survival and mortality during drought: Why do some plants survive while others succumb? *New Phytol.* **178,** 719–739 (2008).
23. Breshears, D. D. *et al.* Tree die-off in response to global-change-type drought: Mortality insights from a decade of plant water potential measurements. *Front. Ecol. Environ.* **7,** 185–189 (2009).
24. Jiang, X. *et al.* Projected future changes in vegetation in western North America in the 21st century. *J. Clim.* **26,** 3671–3687 (2013).
25. Choat, B. *et al.* Global convergence in the vulnerability of forests to drought. *Nature* **491,** 752–755 (2012).
26. Gerald, A. *et al.* The WCRP CMIP3 multimodel dataset: A new era in climate change research. *Bull. Am. Meteorol. Soc.* **88,** 1383–1394 (2007).
27. Rauscher, S. A., Kucharski, F. & Enfield, D. B. The role of regional SST warming variations in the drying of meso-America in future climate projections. *J. Clim.* **24,** 2003–2016 (2011).
28. Allen, C. D., Breshears, D. D. & McDowell, N. G. On underestimation of global vulnerability to tree mortality and forest die-off from hotter drought in the Anthropocene. *Ecosphere* **6,** 129 (2015).
29. Carnicer, J. *et al.* Widespread crown condition decline, food web disruption, and amplified tree mortality with increased climate change-type drought. *Proc. Natl Acad. Sci. USA* **108,** 1474–1478 (2011).
30. Koven, C. D. Boreal carbon loss due to poleward shift in low-carbon ecosystems. *Nature Geosci.* **6,** 452–456 (2013).
31. Settele, J. *et al.* in *Climate Change 2014: Impacts, Adaptation, and Vulnerability* (eds Field, C. B. *et al.*) 271–359 (IPCC, Cambridge Univ. Press, 2014).

Acknowledgements

This work was financially supported by the Department of Energy, Office of Science, by Los Alamos National Lab's Lab Directed Research and Development programme, by NSF-EAR-0724958 and NSF-EF-1340624, and also by ANR-13-AGRO-MACACC, and NSF-IOS-1549959, by the Department of Agriculture AFRI-NIFA programme, by the U.S.G.S. Climate and Land Use Program, and by a National Science Foundation grant to the University of New Mexico for Long Term Ecological Research.

Author contributions

N.G.M. and W.T.P. designed the experiment. A.P.W., C.X., D.S.M., J.O., J.C.D., R.A.F., X.J., J.D.M., S.A.R. and C.K. performed model simulations. N.G.M. performed measurements. L.T.D., S.S., R.P., J.L., J.P. and N.G.M. collected measurements. All authors contributed to the writing of the paper.

Additional information

Supplementary information is available in the online version of the paper. Reprints and permissions information is available online at www.nature.com/reprints. Correspondence and requests for materials should be addressed to N.G.M.

Competing financial interests

The authors declare no competing financial interests.

Addendum: Multi-scale predictions of massive conifer mortality due to chronic temperature rise

N. G. McDowell, A. P. Williams, C. Xu, W. T. Pockman, L. T. Dickman, S. Sevanto, R. Pangle, J. Limousin, J. Plaut, D. S. Mackay, J. Ogee, J. C. Domec, C. D. Allen, R. A. Fisher, X. Jiang, J. D. Muss, D. D. Breshears, S. A. Rauscher and C. Koven

Nature Climate Change **6,** 295–300 (2016); published online 21 December 2015; corrected after print 7 October 2016

Additional details of the estimates of forest mortality from this Letter are required to enhance clarity and reproducibility. First, we wish to clarify what the empirically based projections shown in Figure 3c represent. Unlike process-based model projections that predicted percent tree mortality, our empirically derived mortality projections provide a proxy measure of the cumulative probability of a severe regional mortality event. We defined a severe regional mortality event as a year in which the regionally averaged climate of the Southwest USA (the four-corner states south of 38° N) leads to an estimated predawn plant-water potential value exceeding the mortality threshold, where the estimated predawn plant water potential is based on our empirical equation that uses climate data. Similarly, the projections of mortality based on the Forest Drought Stress Index (FDSI) also represent the cumulative probability of a severe regional mortality event—where a mortality event is assumed to be a year when the FDSI (based on precipitation and vapour-pressure deficit projections in the CMIP5 RCP 8.5 scenario) is more negative than –1.41. This threshold is based on Williams, A. P. *et al.* (*Nat. Clim. Change* **3,** 292–297; 2013), which found –1.41 to be the mean FDSI value during the driest half of years during Southwest USA 'megadrought' events in the 1200s and 1500s, which were associated with widespread forest loss. Figure 3c indicates that the CMIP5-derived probability that such an event has occurred at some point since 1901 converges to 100% in the middle of the twenty-first century for one study species and by the end of the century for the other. These details were not sufficiently clear in our original Methods section.

In contrast, our projections of forest mortality using the process-based models of leaf predawn water potentials allowed predictions of percentage tree mortality. Although most mechanistic model projections indicate a convergence to 100% tree mortality, these models were not provided with the spatial heterogeneity in topography, soil characteristics, competition, and inter-species interactions to allow spatially explicit simulation, but rather provided a range of soil and climate conditions to bracket the full suite of conditions in Southwest USA. Through this permutation of soil properties and climate, the model outputs were used to generate tree mortality at different times over the twenty-first century, providing the step changes in mortality shown in Figure 3c (and explained in the Supplementary Information). Co-occurring substantial increases in the probability of empirically predicted mortality events and per cent tree mortality derived from the mechanistic models are complimentary in their support of one of the main conclusions of our study: that warming-driven increase in aridity are highly likely to lead to substantial increases in Southwest USA conifer mortality throughout the twenty-first century. As is indicated by the spread of the projections, the exact timing of this seemingly inevitable increase is highly uncertain. While it is difficult to determine the exact level of tree mortality that twenty-first century climate change will cause, the most important and realistic feature of the mortality projections shown in Figure 3c is the rapid increase in tree mortality in Southwest USA that may be occurring now and is likely to continue for decades to come, which is supported by multiple independent approaches. An obvious additional step that could be taken for evaluation and application of the empirical and mechanistic models is spatially explicit comparison to inventory data, which will require the use of appropriate (validated) downscaled climate data, additional ancillary data for the mechanistic models (for example, soil depth, aspect and elevation), and careful grouping of the inventory data.

Additionally, we inadvertently provided a preliminary set of equations in the Supplementary Information that were used to estimate water potential based on absolute climate values. These equations were developed during exploratory analysis and were subsequently revised to more comprehensively represent the region by using standardized climate anomalies rather than absolute climate values. The refined equations that were ultimately used were:

$$\text{Pine } \Psi_{pd}\ (\text{April–August}) = -10^{0.0762 - 0.0431\text{zscore}(\log_{10}(\text{ppt})) + 0.0437\text{zscore}(D)}$$

$$\text{Juniper } \Psi_{pd}\ (\text{April–August}) = -10^{0.1195 - 0.0814\text{zscore}(\log_{10}(\text{ppt})) + 0.0606\text{zscore}(D)}$$

Here, Ψ_{pd} is predawn water potential (MPa), ppt is precipitation (mm) total, and D is mean vapour-pressure deficit (kPa). Both variables are evaluated over the 12 months beginning in previous September and ending in the following August. The term 'zscore' indicates that these annual values of $\log_{10}$(ppt) and D are standardized (converted to standard deviation anomalies) relative to the temporal mean and variability of the 1961–2000 period. Units of ppt and D do not matter since these values are standardized within the equations. While these equations are more refined for the region than those previously reported, either set of equations supports our general conclusion that a large increase in Southwest USA tree mortality is likely to occur by 2100.